Mach-Zehnder Interferometer Design for Group Index Characterization in Silicon Photonics

Moshe Technion – Edx - Silicon Photonics Design, Fabrication and Data Analysis

***Abstract*—Silicon photonics has emerged as a leading platform for integrated optical systems, driven by its high integration density, compatibility with CMOS processes, and cost-effective manufacturing. Central to many silicon photonic circuits is the Mach-Zehnder Interferometer (MZI), which exploits wave interference for functions such as switching, modulation, and filtering. This report presents a comprehensive design methodology for MZI structures optimized to experimentally extract the group index of silicon photonic waveguides. By systematically varying the path length differences between MZI arms, the resulting devices exhibit distinct spectral signatures, with the Free Spectral Range (FSR) directly linked to the group index. Finite-difference eigenmode simulations were used to model waveguide dispersion and determine both effective and group indices for a standard 500 nm wide silicon-on-insulator waveguide. The proposed approach enables precise experimental verification of simulated group index values, supporting accurate calibration of photonic design tools and advancing the development of wavelength-sensitive components in silicon photonics.**

I. INTRODUCTION

Silicon photonics represents one of the most promising technological platforms for the next generation of integrated optical systems, offering unique advantages in terms of high integration density, CMOS compatibility, and cost-effective manufacturing [1-3]. The field has seen remarkable growth over the past decade, evolving from academic research into commercial applications spanning telecommunications, data centers, and sensing technologies. The ability to manipulate light at the nanoscale using silicon waveguides has enabled unprecedented miniaturization of optical components while maintaining exceptional performance characteristics.

At the heart of many silicon photonic systems lies the Mach-Zehnder Interferometer (MZI), a versatile optical structure that exploits wave interference phenomena to perform various functions. MZIs serve as fundamental building blocks for optical switches, modulators, filters, and sensing elements. Their operation relies on the precise control of optical path lengths and the resulting phase differences between interfering light waves.

One of the critical parameters governing the behavior of silicon photonic waveguides is the group index, which characterizes how optical pulses propagate through the structure. Unlike the effective refractive index that describes phase velocity, the group index determines the group velocity of light pulses and directly influences the device's spectral response and dispersion properties. Accurate knowledge of the group index is essential for designing wavelength-sensitive components, predicting time delays, and understanding bandwidth limitations in high-speed applications.

This report presents a comprehensive design methodology for silicon photonic MZI structures specifically tailored for experimental extraction of waveguide group index values. By systematically varying the path length differences between the MZI arms, we can create devices with distinct spectral signatures whose Free Spectral Range (FSR) directly correlates to the group index. This approach enables precise experimental verification of simulated values and provides valuable feedback for calibrating photonic design tools.

II. THEORETICAL FOUNDATION

A. Wave Propagation in Silicon Waveguides

The propagation of electromagnetic waves in dielectric waveguides is governed by Maxwell's equations, which, when solved for specific boundary conditions, yield the supported optical modes. Each mode represents a distinct field distribution pattern that maintains its shape while propagating, though its amplitude and phase may evolve.

For silicon waveguides fabricated on silicon-on-insulator (SOI) substrates, the high index contrast between the silicon core ($n \approx 3.45$) and the surrounding silicon dioxide cladding ($n \approx 1.45$) enables strong light confinement in sub-micron dimensions. This confinement leads to enhanced field intensities, nonlinear effects, and dispersion characteristics that distinguish silicon photonics from other optical platforms.

The waveguide's effective index (n_{eff}) represents a weighted average of the refractive indices of the materials through which the optical mode travels, with weights determined by the fraction of optical power in each material. Mathematically, the effective index relates to the propagation constant β through:

$$\beta = \left(\frac{2\pi}{\lambda}\right) \times n_{eff} \quad (1)$$

where λ is the free-space wavelength. The effective index varies with wavelength due to both material dispersion (wavelength dependence of bulk material indices) and geometric dispersion (wavelength-dependent mode confinement).

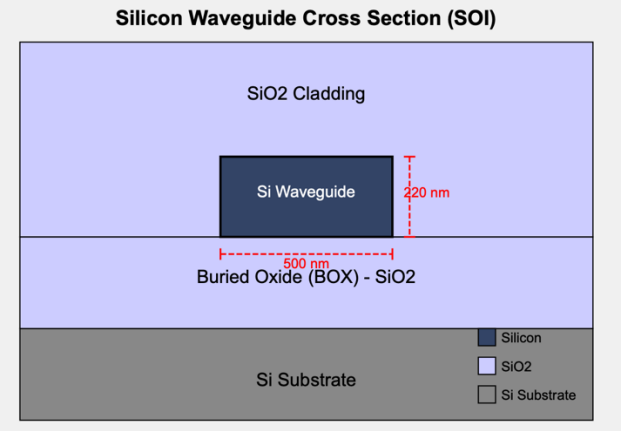

Fig. 1. Cross-section of a silicon-on-insulator (SOI) waveguide. The waveguide consists of a 220 nm thick and 500 nm wide silicon core surrounded by a silicon dioxide (SiO_2) cladding and a buried oxide (BOX) layer on top of the silicon substrate.

While the effective index describes phase evolution, practical optical systems often operate with pulses or modulated signals that span multiple wavelengths. The group index (ng) characterizes how these pulses propagate and is defined as [3,4]:

$$ng = n_{eff} - \lambda \times \left(\frac{dn_{eff}}{d\lambda}\right) \quad (2)$$

This equation incorporates both the effective index value and its wavelength derivative, capturing the combined effects of material and geometric dispersion. The group index is typically higher than the effective index in silicon waveguides due to the negative slope of neff versus wavelength.

For SOI waveguides, the group index has significant implications:

1) It determines the group velocity (vg = c/ng) at which optical pulses travel through the waveguide
2) It affects the chromatic dispersion, which can lead to pulse broadening in high-speed systems
3) It directly influences the free spectral range (FSR) of interferometric and resonant structures
4) It impacts the waveguide's sensitivity to temperature and dimensional variations

Understanding and accurately measuring the group index is therefore essential for predicting timing relationships in complex photonic circuits and designing wavelength-selective components with precise spectral characteristics.

B. Mach-Zehnder Interferometer Principles

The Mach-Zehnder Interferometer represents one of the most fundamental optical structures used in integrated photonics. Its operation relies on the interference between light waves that travel along two separate paths before recombining.

A basic MZI consists of:

1. **Input waveguide** - Carries the incident light to the device
2. **Splitting element** - Divides the input light into two equal parts (commonly implemented as a Y-junction or directional coupler)
3. **Two interferometer arms** - Separate waveguide paths with potentially different lengths or properties
4. **Combining element** - Merges the light from both arms, allowing interference to occur
5. **Output waveguide** - Carries the resulting interference pattern

When a light wave of amplitude E_0 enters the MZI, it is divided into two equal-amplitude waves ($E_0/\sqrt{2}$) at the splitter. After traversing the two arms with optical path lengths L_1 and L_2, the waves acquire phase shifts $\phi_1 = \beta_1 L_1$ and $\phi_2 = \beta_2 L_2$ respectively, where β represents the propagation constant. Upon recombination, the resulting output amplitude depends on the relative phase difference $\Delta\phi = \phi_2 - \phi_1$.

For an ideal symmetric MZI with identical propagation constants ($\beta_1 = \beta_2 = \beta$) and a path length difference $\Delta L = L_2 - L_1$, the output intensity follows [3,5]:

$$I_{out} = \left(\frac{I_{in}}{2}\right) \times [1 + cos(\beta \times \Delta L)] \quad (3)$$

When scanning across wavelengths, the propagation constant β varies, causing the output to oscillate between constructive interference (maximum transmission) and destructive interference (minimum transmission). The wavelength spacing between adjacent transmission maxima defines the free spectral range (FSR) of the MZI and relates directly to the group index:

$$FSR = \frac{\lambda^2}{ng \times \Delta L} \quad (4)$$

This equation reveals the inverse proportionality between FSR and both group index and path length difference, providing the theoretical basis for our group index extraction methodology. By fabricating MZIs with known path length differences and measuring their spectral responses, we can experimentally determine the group index with high precision.

III. Modelling and Simulation

A. Waveguide Design - Structure Selection

For this design course project, I focus exclusively on the strip waveguide configuration with a height of 220 nm, as dictated by the standard SOI wafer specifications and fabrication constraints outlined in the course syllabus. While the original design considered multiple width options, this refined

approach concentrates solely on the 500 nm width waveguide, which represents the industry standard dimension with well-documented optical properties.

The 500 nm width selection offers several advantages:

1. It supports single-mode operation in the C-band (1530-1565 nm) for the fundamental TE mode
2. It provides strong mode confinement while maintaining reasonable bend radii
3. It has been extensively characterized in literature, offering valuable reference points
4. It balances propagation loss with effective light-guiding capabilities
5. It demonstrates moderate sensitivity to fabrication variations compared to narrower waveguides

B. ***Mode Analysis***

I performed comprehensive mode analysis using finite-difference eigenmode (FDE) simulations to characterize the 500 nm waveguide's optical properties across the C-band using commercial eigenmode solver Lumerical [6]. The simulation framework systematically calculated effective index values at multiple wavelengths, enabling accurate determination of the group index through numerical differentiation.

It is important to note that these simulations were specifically conducted for the fundamental Transverse Electric (TE) mode, aligning with the operational requirements and typical polarization used in silicon photonic waveguides.

For the 500 nm wide waveguide at the central wavelength of 1550 nm, the simulation yielded:

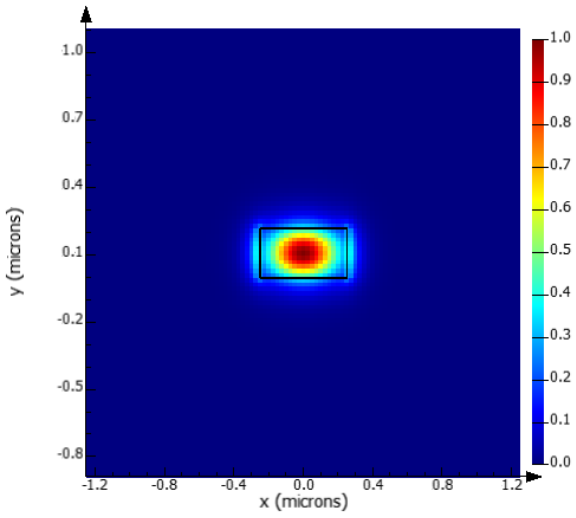

Fig. 2. Simulated mode profile of the first TE mode in the silicon-on-insulator (SOI) waveguide. Effective index (n_{eff})- 2.45 and Group index (ng) - 4.2.

The electric field profile shows strong confinement within the silicon core. The mode exhibits the characteristic asymmetric distribution typical of SOI strip waveguides, with slight field penetration into the underlying oxide layer and more substantial evanescent field extending into the upper cladding.

C. ***Dispersion Modeling***

To accurately characterize the wavelength-dependent behavior of the 500 nm waveguide, I fitted the simulated effective index data with a second-order polynomial model:

$$neff(\lambda) = a_0 + a_1(\lambda - 1.55) + a_2(\lambda - 1.55)^2 \quad (5)$$

where λ is expressed in micrometers, and 1.55μm serves as the reference wavelength. Fig3. Presents the simulation results:

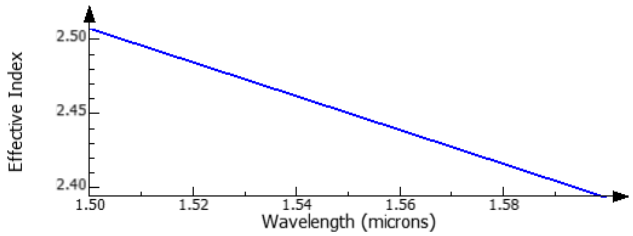

Fig. 3. Mode simulation results for frequency sweep to calculate the dispersion model.

This polynomial model enables analytical calculation of the effective index at any wavelength within the C-band without requiring additional simulations. Furthermore, by taking the derivative of this expression with respect to wavelength, we can directly compute the group index:

$$ng(\lambda) = neff(\lambda) - \lambda \times [a_1 + 2a_2(\lambda - 1.55)] \quad (6)$$

For the 500 nm wide waveguide (TE polarization), the regression analysis yielded the following coefficients:

- a_0 = 2.442 (effective index at 1550 nm)
- a_1 = -1.127 (first-order dispersion term)
- a_2 = -0.034 (second-order dispersion term)

D. ***MZI Circuit Design***

Fig.4 presents the simulated MZI circuit:

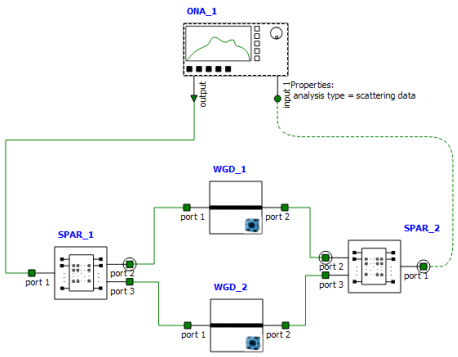

Fig. 4. MZI circuit in INTERCONNET

Simulation results are presented in Fig.5:

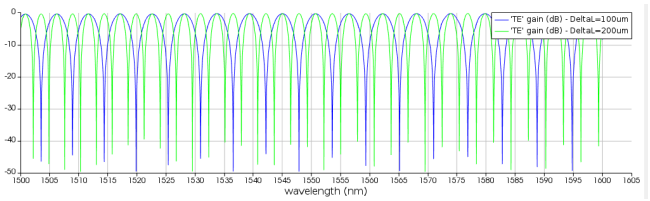

To ensure comprehensive characterization of the group index while meeting the requirement of FSR < 50 nm specified in the course guidelines, I intend to design a series of MZIs with varying path length differences. Each configuration targets a specific spectral signature that enables precise extraction of the group index from experimental measurements. The selected path length differences are:

TABLE I
FSR from simulations VS ΔL

ΔL [µm]	FSR [nm]
40	14.3
80	7.12
120	4.72
160	3.55
180	3.17
200	2.85

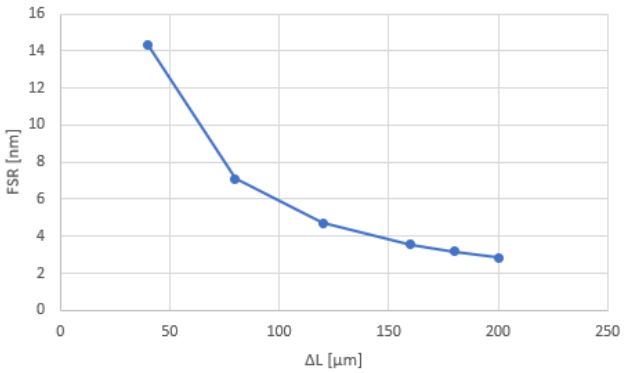

Fig. 5. Simulated FSR as function of ΔL of the MZI circuit

These values provide a good distribution of spectral features while maintaining measurement accuracy.

IV. Fabrication

A. Layout Submission

The experimental design incorporated six Mach-Zehnder Interferometer (MZI) devices with systematically varied path length differences (ΔL). Each MZI configuration comprised two grating couplers and two Y-splitters connecting waveguides of lengths L_1 and L_2. While L_1 was maintained constant at 150 µm across all devices, L_2 was incrementally increased (190 µm, 230 µm, 270 µm, 310 µm, 350 µm, and 550 µm) to investigate the relationship between path length difference and Free Spectral Range (FSR), as illustrated in Fig. 5.

Fig.6. illustrates the layout

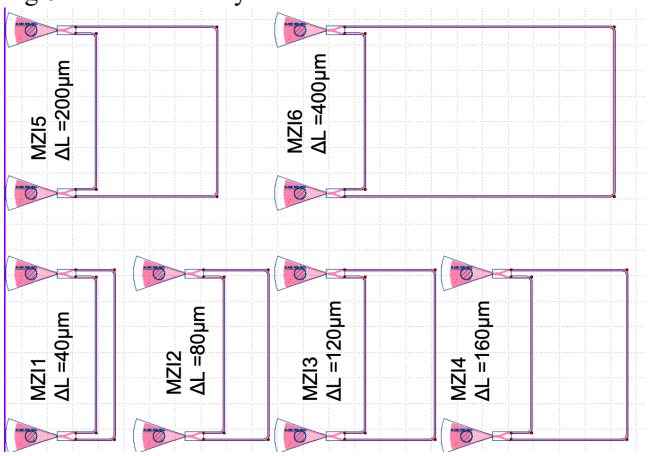

Fig. 6. Layout for the MZIs devices

The photonic devices used in this work were fabricated by Applied Nanotools Inc. (Edmonton, Canada) using their NanoSOI multi-project wafer (MPW) process [7], which is based on 100 keV direct-write electron beam lithography. The process utilized 200 mm silicon-on-insulator (SOI) wafers with a 220 nm device layer and a 2 µm buried oxide layer. Devices were patterned with high precision using a JEOL JBX-8100FS system, and fabrication included proximity effect correction, ICP-RIE etching, and PECVD oxide cladding deposition. The final structures were verified by SEM and reflectometry to ensure dimensional and material accuracy.

V. Analysis

A. Corner Analysis

In this study, we consider fabrication-induced variations in both the wafer thickness and waveguide width. Specifically, the wafer thickness is assumed to range from 215.3 nm to 223.1 nm, while the waveguide width varies between 470 nm and 510 nm. These geometric deviations correspond to an expected operational wavelength range of approximately 4.1759 µm to 4.2517 µm.

TABLE II
Corner analysis for fabrication variations

	Silicon waveguide **thickness** variation [nm]	Silicon waveguide **width** variation [nm]	Simulated group index values for the corner analysis variations
Minimum value	215.3	470	4.1759
Maximum value	223.1	510	4.2517

B. Measurement and Characterization

Device characterization was performed using a custom-built automated test setup with control software written in Python [3,8]. An Agilent 81600B tunable laser served as the input source, and Agilent 81635A optical power sensors were used for output detection. The wavelength was swept from 1500 to 1600 nm in 10 pm increments. **Crucially, the grating couplers, subsequent analysis and simulations were specifically designed for and focused on the Transverse Electric (TE) polarization. This selection ensures efficient coupling and accurate characterization of the fundamental TE mode, which is essential for the targeted waveguide properties and MZI operation in silicon photonics.** Polarization-maintaining (PM) fibers were used to ensure stable TE-mode coupling into the grating couplers. A PM fiber array was employed for efficient coupling of light into and out of the chip.

Different path length differences (ΔL) were simulated and fabricated; however, the detailed analysis in this work focuses on the device with ΔL = 200 µm. A summary of the measurement results for the other devices is also provided for comparison.

Figure 7 shows the measurement results for the MZI with a path length difference of ΔL = 200 µm. To account for variations in the measurement bandwidth, a polynomial fit correction was applied. Figure 7(a) displays the raw, uncorrected bandwidth data along with the fitted polynomial curve, while Figure 7(b) presents the bandwidth after applying the correction.

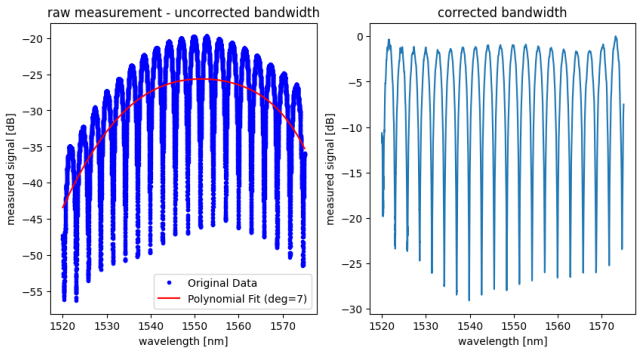

(a) (b)

Fig. 7. Bandwidth measurement results for the Mach–Zehnder Interferometer (MZI) with a path length difference of ΔL = 200 µm. (a) Raw measured bandwidth with overlaid polynomial fit used for correction. (b) Corrected bandwidth after applying the polynomial fit adjustment.

Figure 8 illustrates the corrected transmission spectrum for the MZI with a path length difference of ΔL = 200µm. The plot compares the measured transmission data with the fitted response based on the analytical MZI model described in Equation 3. The strong agreement between the measured and fitted curves validates the accuracy of the model and the parameter extraction process. The periodic interference fringes are well-captured, indicating consistent phase behavior and confirming the reliability of the bandwidth correction and fitting approach.

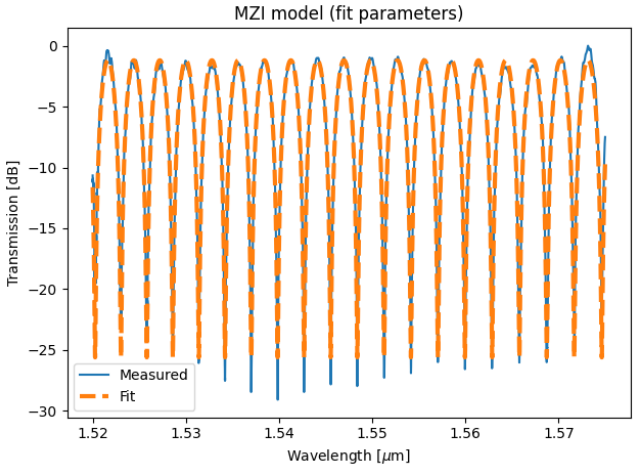

Fig 8. Corrected transmission spectrum of the MZI with ΔL = 200 µm, showing the measured data and the corresponding fit based on the MZI model (Equation 3). The fitted curve accurately captures the interference pattern and confirms the consistency of the extracted parameters

To accurately compare the simulated and measured Mach-Zehnder Interferometer (MZI) responses, an autocorrelation phase shift was applied to the simulation data. This correction was necessary because fabrication imperfections (such as slight variations in waveguide dimensions or material properties) and environmental factors (like temperature fluctuations during measurement) introduce an inherent phase offset in the fabricated device that is not accounted for in an ideal simulation. By applying this phase shift, we ensure that the simulated and measured interference patterns align, allowing for a direct and valid comparison of the MZI's designed spectral characteristics (e.g., Free Spectral Range and extinction ratio). Figure 9 illustrates the comparison between the measured data and the Lumerical Interconnect simulation results for the MZI with ΔL = 200 µm.

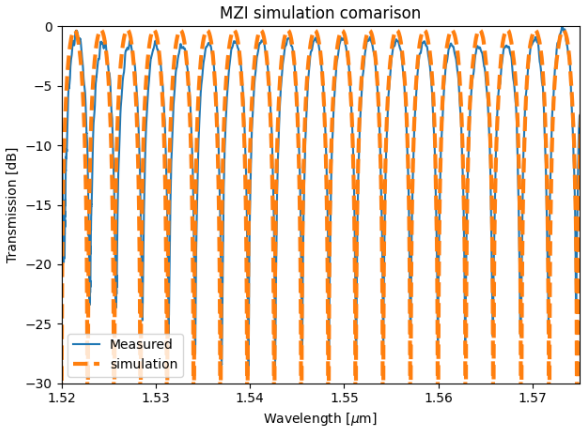

Fig 9. Comparison between the measured data and the Lumerical Interconnect simulation results for the MZI with ΔL = 200 µm.

The effective index was extracted from the measured MZI results using the Mean Squared Error (MSE) method. Subsequently, the group index was calculated from this effective index via Equation

2, yielding a value of **4.1822**. This calculated group index, validated through a Python script, aligns well with the corner analysis (see Table II), confirming excellent agreement between measurements, simulations, and the MZI's analytical model.

Table III and Figure 10 summarize the comparison between simulated and measured results for the Mach-Zehnder Interferometer (MZI) devices with varying path length differences (ΔL). Table III presents the Free Spectral Range (FSR) values obtained from both simulations and measurements, along with the group index calculated from the measurements for different ΔL values. For instance, for a ΔL of 40 µm, the simulated FSR is 14.3 nm, while the measured FSR is 14.4 nm, resulting in a calculated group index of 4.165. Similarly, for a ΔL of 200 µm, the simulated FSR is 2.85 nm, and the measured FSR is 2.88 nm, with a calculated group index of 4.182. It is noted that the MZI with ΔL = 180 µm was "Not sent to fabrication". Figure 10 visually represents this data, plotting the FSR against ΔL for both simulation and measurement results. The close alignment between the simulated and measured data points in both the table and the graph indicates strong agreement between the theoretical models, simulations, and experimental results. This agreement validates the accuracy of the MZI model and the group index extraction methodology.

Simulation VS measurements:

TABLE III
Measurement and simulation results summary

ΔL [µm]	FSR from simulations [nm]	FSR from measurements [nm]	Group index calculated from measurements
40	14.3	14.4	4.165
80	7.12	7.2	4.172
120	4.72	4.8	4.174
160	3.55	3.6	4.175
180	3.17	Not sent to fabrication	
200	2.85	2.88	4.182
400	1.42	1.43	4.182

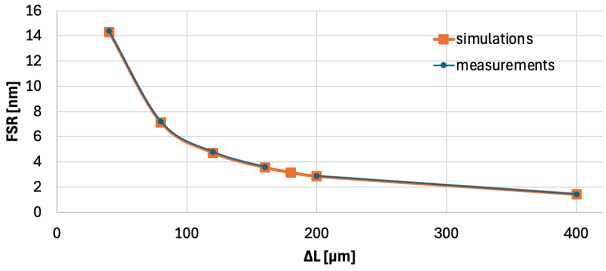

Fig 10. FSR VS the path differences of the MZI: simulation and measurement results.

VI. Conclusions

This report presents a comprehensive design methodology for Mach-Zehnder Interferometer (MZI) structures optimized for experimentally extracting the group index of silicon photonic waveguides. Silicon photonics is a leading platform for integrated optical systems due to its high integration density, compatibility with CMOS processes, and cost-effective manufacturing. The MZI is a central component in many silicon photonic circuits, utilized for switching, modulation, and filtering through wave interference. Accurate knowledge of the group index is crucial for designing wavelength-sensitive components, predicting time delays, and understanding bandwidth limitations in high-speed applications.

The design methodology involved systematically varying the path length differences between the MZI arms, which creates distinct spectral signatures where the Free Spectral Range (FSR) is directly linked to the group index. Finite-difference eigenmode (FDE) simulations were employed to model waveguide dispersion and determine both effective and group indices for a standard 500 nm wide silicon-on-insulator (SOI) waveguide. For a 500 nm wide waveguide at 1550 nm, the simulation yielded an effective index (neff) of 2.45 and a group index (ng) of 4.2.

Fabrication of the devices was performed by Applied Nanotools Inc. using 100 keV direct-write electron beam lithography on 200 mm SOI wafers with a 220 nm device layer. Six MZI devices with varying path length differences (ΔL) were incorporated, with L1 constant at 150 µm and L2 incrementally increased from 190 µm to 550 µm. The experimental characterization used an automated test setup with an Agilent 81600B tunable laser and Agilent 81635A optical power sensors, sweeping wavelengths from 1500 to 1600 nm.

The results demonstrated excellent agreement between simulations and measurements. For the MZI with ΔL = 200 µm, the measured transmission spectrum closely matched the fitted analytical MZI model. Furthermore, after applying an autocorrelation phase shift to account for fabrication imperfections, the measured data aligned well with Lumerical Interconnect simulation results. The group index calculated from the measured MZI results using the Mean Squared Error (MSE) method was 4.1822 , which aligns well with the simulated corner analysis values ranging from 4.1759 to 4.2517 for fabrication variations. This proposed approach enables precise experimental verification of simulated group index values, supporting accurate calibration of photonic design tools and advancing the development of wavelength-sensitive components in silicon photonics.

Acknowledgements

I acknowledge the *edX UBCx Phot1x: Silicon Photonics Design, Fabrication, and Data Analysis* course, supported by the Natural Sciences and Engineering Research Council of Canada (NSERC) through the SiEPIC (Silicon Electronic-Photonic Integrated Circuits) Program. I want to acknowledge course instructors Prof. Lukas Chrostowski and Mateo Branion-Calles. I also acknowledge the use of design software from Lumerical and KLayout.

REFERENCES

[1] Reed, G. T., & Knights, A. P. (2004). Silicon Photonics: An Introduction. Wiley.
[2] Soref, R. A. (2006). "The past, present, and future of silicon photonics." *IEEE Journal of Selected Topics in Quantum Electronics*, 12(6), 1678–1687.
[3] Lukas Chrostowski, Michael Hochberg, chapter 12 in "Silicon Photonics Design: From Devices to Systems", Cambridge University Press, 2015
[4] Bogaerts, W. et al., "Silicon microring resonators," *Laser & Photonics Reviews*, 6(1), 47–73 (2012)
[5] Saleh & Teich, *Fundamentals of Photonics*
[6] Lumerical documentation: https://optics.ansys.com (for FDE solver)
[7] Applied Nanotools or the NanoSOI MPW process. https://www.appliednt.com
[8] http://mapleleafphotonics.com, Maple Leaf Photonics, Seattle WA, USA.